A Phase II Study of Cabozantinib and Androgen Ablation in Patients with Hormone-Naïve Metastatic Prostate Cancer

Paul G. Corn[1], Miao Zhang[2], Graciela M. Nogueras-Gonzalez[3], Lianchun Xiao[3], Amado J. Zurita[1], Sumit K. Subudhi[1], Shi-Ming Tu[1], Ana M. Aparicio[1], Cristian Coarfa[4], Kimal Rajapakshe[4], Shixia Huang[5], Nora M. Navone[6], Sue-Hwa Lin[6], Guocan Wang[1], Sumankalai Ramachandran[1], Mark A. Titus[1], Theocharis Panaretakis[1], Gary E. Gallick[1,†], Eleni Efstathiou[1], Patricia Troncoso[2], and Christopher Logothetis[1]

ABSTRACT

Purpose: Cabozantinib, an oral inhibitor of c-MET/VEGFR2 signaling, improved progression-free survival (mPFS) but not overall survival (OS) in metastatic castrate-resistant prostate cancer. We evaluated cabozantinib plus androgen deprivation therapy (ADT) in hormone-naïve metastatic prostate cancer (HNMPCa).

Patients and Methods: Patients received ADT plus cabozantinib starting at 60 mg daily. The primary endpoint was castrate-resistant PFS by radiographic criteria, clinical progression, or receipt of additional therapy. Secondary endpoints included OS, safety, radiographic responses, and biomarker modulation.

Results: Sixty-two patients received treatment. With a median follow-up of 31.2 months, the mPFS was 16.1 months (95% CI, 14.6–22.7 months), and mOS was not reached. Reductions in PSA $\geq$ 90%, bone-specific alkaline phosphatase $\geq$ 50%, and urine N-

telopeptides $\geq$ 50% occurred in 83%, 87%, and 86% of evaluable patients, respectively. Responses in bone scan and measurable disease were observed in 81% of and 90% of evaluable patients, respectively. Most common grade 3 adverse events were hypertension (19%), diarrhea (6%), and thromboembolic events (6%), and dose reductions occurred in 85% of patients. Analysis of baseline cytokine and angiogenic factors (CAFs) revealed that higher plasma concentrations of Lumican, CXCL5, CD25, and CD30 were associated with shorter PFS as was high tumor expression of pFGFR1.

Conclusions: Cabozantinib plus ADT has promising clinical activity in HNMPCa. CAF profiles and tissue markers suggest candidate prognostic and predictive markers of cabozantinib benefit and provide insights for rational therapy combinations.

Introduction

Cabozantinib, an oral small-molecule inhibitor of c-MET/VEGFR2 signaling, elicits unprecedented responses in bone scans in patients with metastatic castrate-resistant prostate cancer (mCRPC) without correlative changes in PSA (1). Promising results from phase II studies prompted a large randomized, placebo-controlled phase III trial (COMET-1) of cabozantinib in patients with mCRPC after progression on docetaxel and abiraterone and/or enzalutamide. Unfortunately, despite a significant improvement in progression-

free survival (PFS), cabozantinib failed to improve overall survival (OS; ref. 2). Potential reasons for this outcome include the absence of predictive biomarkers for patient enrichment, drug resistance, the possibility that the therapeutic benefit of c-MET/VEGR2 inhibition would be enhanced in earlier disease states, and the probable necessity for combinatorial strategies to optimize cabozantinib efficacy.

Our group has used preclinical and coclinical models as a strategy to provide insights into the clinical findings (3–5). We demonstrated previously that bone scan responses were associated with the direct effects of cabozantinib on osteoblasts and c-MET/VEGFR2 target-inhibition in endothelial cells rather than sustained reduction of prostate cancer epithelial cell growth. Reflecting this, viable prostate cancer epithelial cells expressing activated phospho-Met persist within areas of bone scan improvement (4). We have elucidated several resistance mechanisms that may account for this observation including secretion of survival factors by tumor-induced bone, vascular heterogeneity, and FGF/FGFR signaling (3–5). Because elucidating resistance mechanisms can lead to novel treatment strategies, we have interpreted the aggregate clinical and preclinical activity of cabozantinib as a signal of potent efficacy worthy of further study despite the negative phase III results.

Androgen receptor (AR) signaling represses c-MET expression and androgen deprivation induces c-MET expression in prostate cancer cells, supporting a role for c-MET signaling in the evolution of castrate resistance (6, 7). c-MET expression levels increase during prostate cancer progression with highest levels in bone, the predominant site of advanced lethal disease (8, 9). Inhibition of c-MET significantly reduced the proliferation of prostate cancer cells after castration in orthotopic models (10). Collectively, these data suggest the hypothesis that combining c-MET/VEGFR2 inhibition with androgen

[1]Department of Genitourinary Medical Oncology, The University of Texas MD Anderson Cancer Center, Houston, Texas. [2]Department of Anatomical Pathology, The University of Texas MD Anderson Cancer Center, Houston, Texas. [3]Department of Biostatistics, The University of Texas MD Anderson Cancer Center, Houston, Texas. [4]Department of Molecular and Cellular Biology, Baylor College of Medicine, Houston, Texas. [5]Department of Molecular and Cellular Oncology, Baylor College of Medicine, Houston, Texas. [6]Department of Translational Molecular Pathology, The University of Texas MD Anderson Cancer Center, Houston, Texas.

Note: Supplementary data for this article are available at Clinical Cancer Research Online (http://clincancerres.aacrjournals.org/).

†Deceased.

Corresponding Author: Paul G. Corn, The University of Texas MD Anderson Cancer Center, 1515 Holcombe Boulevard, Houston, TX 77030. Phone: 713-563-7208; Fax: 713-563-0099; E-mail: pcorn@mdanderson.org

Translational Relevance

Despite progress in treatment, metastatic prostate cancer remains an incurable disease. Given the importance of the bone microenvironment in progression, therapeutic strategies that target bone stromal cells in addition to the cancer epithelial cell remain an important area of investigation. Cabozantinib, an oral small-molecule inhibitor of c-MET/VEGFR2 signaling, elicits unprecedented bone scan responses and clinically significant pain relief but failed to improve overall survival in patients with metastatic castrate-resistant prostate cancer. To explore the hypothesis that cabozantinib could delay the onset of castrate resistance, we combined cabozantinib with androgen deprivation therapy in patients with hormone-naïve metastatic prostate cancer. We observed promising anti-disease activity and identified blood and tissue-based markers to potentially identify patient subsets most likely to benefit. These data suggest that moving cabozantinib earlier in the disease course with more potent epithelial-targeting agents such as abiraterone or docetaxel could serve as a foundation to explore rational therapy combinations.

deprivation therapy (ADT) would delay the development of castrate-resistant disease.

To test this hypothesis clinically, we conducted a trial combining ADT with cabozantinib as first-line therapy in patients with newly diagnosed, hormone-naïve metastatic prostate cancer (HNMPCa) using time to castrate resistance as a primary endpoint (Clinical-Trials.gov identifier: NCT01630590). We focused on patients with high-volume disease based on prior studies from our group and others showing that extent of disease at the time of ADT initiation was strongly related to outcome (11, 12). We used an integrated strategy that analyzed blood and tumor tissues to interrogate biological domains implicated in prostate cancer progression as well as response and resistance to cabozantinib. These domains included AR signaling, the bone microenvironment, and cabozantinib-mediated regulation of the immune system. This prospective study builds on our experience of studying prostate cancer bone metastases clinically and coclinically to elucidate mechanism of drug action to inform priority therapy interventions for further investigation.

Patients and Methods

Patients, treatment, and study procedures

Institutional review board approval was obtained for the trial protocol (Supplementary Data), and all patients gave written informed consent. The study was conducted in accordance with ethical principles founded in the Declaration of Helsinki. Eligible patients were men ≥18 years of age, ECOG ≤ 2 with pathologically confirmed adenocarcinoma without small cell elements and metastatic disease assessed by bone scan, CT scan and/or MRI. ADT consisted of LHRH agonist or antagonist therapy. Antiandrogens could be used up to 4 weeks at the beginning of ADT treatment to prevent flare. Up to 3 months of ADT prior to study enrollment was permitted. Patients received cabozantinib orally at a starting dose of 60 mg daily. Dose reductions to 40 and 20 mg daily were permissible per the original protocol (December 13, 2014). To further increase safety and tolerability, the protocol was amended (February 15, 2015) to permit dose interruptions (up to 3 days per week) and utilization of a 2 weeks on, 1 week off alternative schedule, a strategy our group has previously used to increase the

tolerability of sunitinib in metastatic kidney cancer (13, 14). To calculate the dose intensity of cabozantinib, we first multiplied the number of days from the start of therapy to end of therapy by the standard 60-mg dose. We then calculated the actual dose received. The time that a patient was on treatment was divided into periods defined by dates of dose changes, alterations in schedule, and treatment interruptions. The number of days at each dose and schedule minus interruptions was multiplied by the dose the patient received during that period. Dose intensity was equal to the actual dose divided by the ideal dose $\times$ 100 (i.e., expressed as a percentage; ref. 15). Adverse events were graded according to CTCAE Version 4.0. Patients were treated until disease progression, unacceptable toxicity, patient withdrawal, radiation to more than one site, and/or determination by the treating physician that further treatment would not be in the best interest of the patient.

Imaging studies (bone scan, CT scan, and/or MRI) were repeated at week 12, and every 12 weeks thereafter or earlier if suspected progression. Responses in soft-tissue measurable disease were investigator assessed per RECIST 1.1. Bone scans were assessed by radiologists blinded to clinical outcome. Responses were evaluated qualitatively. A "partial" response referred to a bone scan with the report describing interval improvement as evidenced by reduction in intensity of lesions but with the baseline lesions still visible. A "complete" response referred to a bone scan with no scintigraphic evidence of metastatic disease. Trans-iliac bone marrow biopsies and aspirates were collected at baseline. PSA, bone-specific alkaline phosphatase (BAP), and urine n-telopeptides (uNTx) were measured every 6 weeks. Blood for cytokine and angiogenic factor (CAF) analysis was collected at baseline and at 6 weeks on treatment. Blood for steroid measurements was collected during daytime clinic hours on nonfasting blood samples at baseline, every 3 weeks up to week 12, and every 6 weeks thereafter.

Statistical considerations

The primary endpoint of this phase II study was castrate-resistant PFS. Prior data from our institution showed that the median time to castrate-resistant progression using a composite endpoint (increasing PSA, new lesions, worsening symptoms, or receipt of additional therapy) in unselected patients treated with androgen ablation alone was approximately 24 months. However, in a subset of patients with "high-volume" disease (≥3 bone lesions and/or visceral metastases), the median time to progression was 11.2 months (11). The study enrolled all eligible patients regardless of volume status, but we focused on high-volume patients. If the trial continued to maximum accrual and maintained sufficient follow-up to observe 49 progression events with a median PFS (mPFS) of 11.2 months, we estimated that a 95% credible interval for the mPFS would range from 8.5 to 14.9 months with a sample size of 60 patients. The study used a Bayesian model to monitor the trial with a recommendation to stop the trial if the mPFS was worse than historical data. For analysis, we reported the mPFS for the entire cohort and for each of the high- and low-volume groups separately. There was no power calculation for a formal comparison on the primary endpoint between subgroups.

Castrate-resistant progression was defined by any of the following: (i) radiographic progression (using RECIST 1.1 for visceral disease and PCWG2 for bone scans), (ii) receipt of additional anticancer systemic therapy, or (iii) clinical progression warranting discontinuation from the study as judged by the treating physician. The time to progression for the intent-to-treat population was calculated from the start of ADT, not from the date of cabozantinib initiation. Patients alive and free of progression at their last follow-up were censored on that date. For the primary analysis, the Kaplan–Meier product limit method was used to

estimate the mPFS along with the 95% confidence interval for the entire cohort and for each of the high- and low-volume groups separately.

Secondary endpoints included radiographic responses, OS, and biomarker modulation in blood and tumor tissues. Descriptive statistics were used to summarize efficacy of responses in PSA, BAP, uNTx, and RECIST. Responses in BAP and uNTx were reported in patients only with levels above normal at baseline prior to starting cabozantinib.

Biomarkers
Immunohistochemistry
Bone marrow biopsy specimens were obtained and evaluated for tumor content using hematoxylin and eosin staining. Sections with >5% tumor involvement were sectioned to 5 μm and stained with primary antibodies against phospho-FGFR1 (dilution1:100, Cell Signaling Technology Inc.), CD31 antibody (dilution 1:50, Cell Signaling Technology Inc.), AR N-terminus (dilution 1:50, Dako), Ki67 (dilution 1:50, Dako), AR-V7 (dilution 1:500, Remab Biosciences), glucocorticoid receptor (dilution 1:300, BD Biosciences), NKX3.1 (dilution 1:500, Athena Enzyme Systems), phospho-MET (dilution 1:175) (Novus, Littleton, CO, USA), Ki67 (dilution 1:50) (Dako, Carpinteria, CA, USA), and CYP17A1 (dilution 1:300, Novus Biologicals). Marker expression was assessed by scoring two or more fields containing at least 100 tumor cells and expressed as a percentage of involvement and intensity. Pathologists were blinded to clinical outcome. Univariate Cox proportional hazards regression was used to identify associations with each of the markers and mPFS.

Steroid analysis
Steroids were analyzed using liquid chromatography as described previously (16).

CAF analysis
Blood plasma for CAF analysis was collected at baseline and at 6 weeks on treatment and stored at −80°C. Custom multiplex assays to measure select bone microenvironment related markers (Lumican and Galectin-1) were manufactured by EMD Millipore. Commercial kits for additional bone and angiogenic markers were obtained from EMD Millipore (HCMBMAG-22K, TGFBMAG-64K, HIGFMAG-52K, and HANG2MAG-12K), and immunologic markers were measured using a commercially available kit from Invitrogen (EPX650-10065-901). CAF concentrations were measured at the antibody-based proteomics core at Baylor College of Medicine (Houston, TX). All analyses were done from a single-thawed sample, each sample was analyzed in duplicate, and the analysis was blinded to clinical outcome. Following conventions previously established by our group, CAFs with >25% out-of-range (OOR) samples were omitted from the analysis, above-range OOR values were replaced with the highest measured value for the corresponding CAF, and below-range OOR values were replaced by the lowest value on the standard curve divided by half (17). Using these criteria, 8 of 98 CAFs (8.2%) were rejected owing to the number of OOR samples. A total of 90 CAFs were analyzed and included in statistical analyses correlating with clinical outcomes.

For the analysis of CAFs, Wilcoxon matched-pairs signed-ranks test was used to test for differences between the baseline and 6 week measurements. To adjust for multiple testing, we used a false discovery rate to determine which P values were statistically significant whereas controlling the type I error. Classification and regression tree (CART) analysis was used to determine cutoff points for the markers. If a cutoff was not found, the median was used for the analysis as described previously (18). Cox proportional hazards models were used to identify

associations between baseline clinical variables (age, LDH, BAP, ECOG, disease volume, Gleason score, treatment to the primary tumor, bone only, lymph node, and/or visceral involvement), CAFs, and PFS. The multivariate analysis included any baseline clinical variables or CAFs with P < 0.05 in the univariate analysis. A reduced model was found using backward elimination methods at a significance level of P < 0.05.

Results
From January 27, 2014, and January 12, 2016, 62 patients were enrolled and treated, 46 (74%) with *de novo* metastatic disease and 54 (87%) with high-volume disease (**Table 1**). At the time of data

Table 1. Patient characteristics.

N	62
Characteristic	
Age, years	
Median	62
Range	(47–84)
Race, no. of patients (%)	
Caucasian	57 (92)
African American	1 (2)
Hispanic	4 (6)
ECOG performance status, N (%)	
0	45 (73)
1	17 (27)
2	0
Treatment of primary tumor, N (%)	
No	46 (74)
Yes	16 (26)
Gleason score of primary, N (%)	
Unknown	5 (8)
≤7	10 (16)
7 + tertiary 5	2 (3)
8–10	45 (73)
PSA (ng/mL)	
Median	64.7
Range	(1.2–2, 131.6)
LDH, IU/L (nl 313–618)	
Median	469.5
Range	(296.0–1,197.0)
Bone-specific alkaline phosphatase, μg/L (nl < 20)	
Patients with baseline value, N (%)	59 (95)
Median	61
Range	(8.4–2,000)
Bone metastases, N (%)	58 (94)
Bone only, N (%)	27 (44)
Visceral metastases, N (%)	8 (13)
Soft-tissue metastases, N (%)	
None	29 (47)
Lymph nodes	33 (53)
Liver	2 (3)
Lung	6 (10)
^aVolume of metastases, N (%)	
Low	8 (13)
High	54 (87)
Time from start of ADT to cabozantinib, weeks	
Median	3.3
Range	0–11.9
Bone strengthening agents, N (%)	
None	51 (82)
Zolendronic acid	3 (5)
Denosumab	8 (13)

[a]≥3 bone lesions and/or visceral involvement.

capture (June 28, 2018), 57 (92%) had discontinued study drug and 50 (81%) had developed castrate-resistant progression. The median time from the start of ADT to the start of cabozantinib was 3.3 weeks (range, 0–11.9 weeks). Reasons for cabozantinib discontinuation included disease progression in 37 (65%), toxicity in 9 (16%), patient withdrawal related to study treatment in 2 (3%), patient withdrawal unrelated to study treatment in 2 (3%), treatment to maximal benefit in 4 (7%), detection of a second primary tumor in 2 (3%), and a motor vehicle accident in 1 (2%). In the 4 patients treated to maximal benefit, 3 had presented with *de novo* metastatic disease and after maximal response in bone (1 with a complete response and two with a partial response) were offered radical prostatectomy.

The median duration of cabozantinib treatment was 13.8 months (95% CI, 10.5–15.7 months). Dose reductions occurred in 53 (85%) patients. Forty-two (68%) were reduced to 40 mg and of these, 11 (18%) were further reduced to 20 mg. The median time to the first dose reduction was 2.1 months (range, 0.7–11.3), and the median time to the second dose reduction was 5.7 months (range, 2.1–11.7). Alterations in dosing schedule occurred in 27 (44%) patients. Seventeen (27%) were altered to a 5-day on/2-day off schedule (13 patients at 40 mg and 4 patients at 20 mg), 9 (15%) were altered to a 4-day on/3-day off schedule (7 patients at 40 mg and 2 patients at 20 mg) and 1 (2%) was altered to 2-week on/1-week off schedule (at 40 mg). The median dose intensity was 69% (range, 25–100).

With a median follow-up of 31.2 months, the mPFS was 16.1 months (95% CI, 14.6–22.7 months) for the entire group, 16.1 months (95% CI, 13.3–21.5 months) for the high-volume group and 20.2 months (95% CI, 15.1–NA months) for the low-volume group (HR 1.56; 95% CI, 0.66–3.66, $P = 0.31$). In the 50 patients who had progressed, criteria for progression were radiographic in 41 (82%), receipt of additional systemic therapy in 7 (14%), and clinical in 2 (4%). The median radiographic PFS was 17.9 months (95% CI, 15.6–26.9 months) for the entire group, 17.9 months (95% CI, 14.9–26.9 months) for the high-volume group, and 24.5 months (95% CI, 15.6–NA months) for the low-volume group (HR, 1.76; 95% CI, 0.63–4.95, $P = 0.285$). Eighteen (29%) patients have died with median OS not yet reached.

Reductions in PSA > 90%, BAP > 50% and urine N-telopeptides > 50% occurred in 50 of 60 (83%), 34 of 39 (87%), and 18 of 21 (86%) of evaluable patients, respectively (Supplementary Fig. SA1a–SA1c). Bone scans were evaluable in 54 patients with partial responses in 34 of 54 (63%) and complete responses in 10 of 54 (19%; Supplementary Fig. SA1d). In evaluable patients with RECIST measurable disease ($n = 30$), best response was stable disease in 3 of 30 (10%), partial response in 18 of 30 (60%), and complete response in 9 of 30 (30%; Supplementary Fig. SA1e).

Treatment-related adverse events (AE) are described in **Table 2**. The most common grade 3 AEs included hypertension in 12 (19%), diarrhea in 4 (6%), and thromboembolic events in 4 (6%). In the 9 patients who discontinued treatment related to AEs, 2 (3%) did so for a stroke, 1 (2%) for transient-ischemic attack, 1 (2%) for pulmonary embolism, 1 (2%) for proteinuria, 1 (2%) for peripheral neuropathy, 1 (2%) for nausea and emesis, 1 (2%) for diarrhea, and 1 (2%) for hypertension and gait disturbance. There were no grade 4 AEs or treatment-related deaths.

Tissue analysis

Trans-iliac bone marrow biopsies were performed on 50 (81%) patients prior to start of cabozantinib, and image-guided bone biopsies were available on 4 (6%) additional patients. Twenty-one (34%) yielded >5% tumor involvement sufficient for IHC analysis. The median time from start of ADT to biopsy was 3.1 weeks. Nuclear AR and NKX.1 expression varied in involvement and intensity but were present in the majority of baseline bone tumor biopsies. Heterogeneous expression of CYP17 was present in ~40% of cases (including 4 patients prior to ADT exposure). Univariate Cox proportional hazards regression analysis revealed that higher expression levels of phospho-Met, CD31, phospho-FGFR1 (a marker of activated FGF/FGFR signaling), and Ki67 were associated with a shorter mPFS (**Table 3**). Supplementary Fig. SA2 shows representative examples of IHC staining for each marker.

Blood steroid measurements

Baseline testosterone, androstenedione, and cortisol (nonfasting) levels prior to start of cabozantinib and serial measurements on treatment were available for 58 (94%) patients. Median nadirs on treatment were 2.5 ng/dL (range, 0.3–9.0), 4.0 ng/dL (range, 0.4–18.4), and 0.7 µg/dL (range, 0.1–5.6) for testosterone, androstenedione, and cortisol, respectively. The median time to nadir measurements after start of ADT were 8.8 months (range, 1.5–25.8), 8.4 months (range, 1.2–23.9), and 7.2 months (range, 1.4–26.8) for testosterone, androstenedione, and cortisol, respectively. By univariate analysis, lower nadirs of each steroid were associated with a longer mPFS (Supplementary Table SA1).

Analysis of CAFs

Plasma samples were available on 60 (97%) patients at baseline and 54 (87%) patients at 6 weeks. Median baseline and 6 week CAF concentrations for all 90 CAFs are listed in Supplementary Table SA2. We focused on CAFs involved in pathways implicated in cabozantinib mechanism of action, resistance to cabozantinib, and immunomodulatory effects of cabozantinib. Using an α level of 0.01, 33 (37%) CAFs demonstrated significant differences in median concentrations between baseline and 6 weeks (**Table 4**; Supplementary Fig. SA3).

Angiogenesis

Significant elevations in VEGF-A and PLGF occurred in combination with a reduction in Angiopoietin-2, changes consistent with cabozantinib-mediated inhibition of VEGF/VEGFR2-regulated angiogenesis.

Bone stromal factors

Bone stromal–derived factors implicated in resistance to cabozantinib include integrin ligands, growth factors, and modulators of osteoblast function. After 6-week treatment, a mixed pattern was observed, with significant elevations in several (IGF-2, galectin-3, and tenascin C) and significant reductions in others (periostin, osteonectin, osteopontin, CCL8, and IGFBP-2).

Immunomodulation

Immunomodulatory CAFs were divided broadly into two categories: (i) those that enhance MDSC, tumor-associated macrophage (TAM), and/or T-regulatory (Treg) function to antagonize an antitumor immune response, including TH2 and M2 cytokines ("immune-inhibitory") and (2) those that antagonize MDSC, TAM, and/or Treg function to promote an antitumoral immune response, including TH1 and M1 cytokines ("immune-stimulatory"). Twelve of 24 (50%) of immune-inhibitory CAFs demonstrated statistically significant declines following 6 weeks of cabozantinib treatment including interleukins (e.g., IL1α and IL23), chemokines (e.g., CCL22 and CXCL11), and growth factors (e.g., M-CSF). In contrast, 1 of 8 (13%) immune-stimulatory CAFs demonstrated a significant decline (IL15). Median

Table 2. Therapy-associated toxicities, number of patients (%).

	All grades	Grade 1	Grade 2	Grade 3	Grade 4
Clinical					
Abdominal pain	8 (13)	4 (6)	4 (6)	1 (2)	0
Alopecia	13 (21)	13 (21)	0	0	0
Anorexia	16 (26)	11 (18)	5 (8)	0	0
Constipation	27 (44)	24 (39)	2 (3)	1 (2)	0
Cough	12 (19)	12 (19)	0	0	0
Diarrhea	45 (73)	28 (45)	13 (21)	4 (6)	0
Dry skin	18 (29)	17 (27)	1 (2)	0	0
Dysgeusia	36 (58)	32 (52)	4 (6)	0	0
Dyspnea	20 (32)	17 (27)	1 (2)	2 (3)	0
Fatigue	56 (90)	30 (48)	24 (39)	2 (3)	0
Gastroesophageal reflux	17 (27)	6 (10)	11 (18)	0	0
Hematuria	5 (8)	3 (5)	1 (2)	1 (2)	0
Hoarseness	20 (32)	19 (31)	1 (2)	0	0
Hypertension	24 (39)	3 (5)	9 (15)	12 (19)	0
Hypothyroidism	39 (63)	13 (21)	26 (42)	0	0
Mucositis	18 (29)	7 (11)	11 (18)	0	0
Nausea	31 (50)	21 (34)	9 (15)	1 (2)	0
Palmar-plantar syndrome	31 (50)	14 (23)	17 (27)	0	0
Pancreatitis	2 (3)	0	1 (2)	1 (2)	0
Peripheral neuropathy	5 (8)	4 (6)	1 (2)	0	0
Rash	11 (18)	9 (15)	2 (3)	0	0
Thromboembolic event	5 (8)	0	1 (2)	4 (6)	0
Vomiting	14 (23)	9 (15)	5 (8)	0	0
Laboratory					
Elevated ALT	51 (82)	42 (68)	6 (10)	3 (5)	0
Anemia	53 (85)	49 (79)	3 (5)	1 (2)	0
Elevated AST	50 (81)	43 (69)	4 (6)	3 (5)	0
Elevated bilirubin	11 (18)	9(15)	2 (3)	0	0
Elevated glucose	47 (76)	34 (55)	11 (18)	2 (3)	0
Hypoalbuminemia	20 (32)	17 (27)	3 (5)	0	0
Hypocalcemia	11 (18)	6 (10)	5 (8)	0	0
Hypomagnesemia	30 (48)	29 (47)	1 (2)	0	0
Elevated lipase	16 (26)	10 (16)	3 (5)	3 (5)	0
Reduced neutrophils	21 (34)	16 (26)	3 (5)	2 (3)	0
Reduced platelets	26 (42)	26 (42)	0	0	0
Proteinuria	44 (71)	40 (65)	3 (5)	1 (2)	0

fold changes on treatment were generally more pronounced for immune-inhibitory CAFs compared with immune-stimulatory CAFs, with the exception of sAXL (Supplementary Fig. SA3).

Univariate analysis of relevant baseline clinical variables and all 90 CAFs to mPFS is shown in Supplementary Table SA3. For baseline clinical variables, only higher BAP levels were associated with shorter mPFS, whereas age, performance status, PSA, LDH, Gleason score, prior definitive local therapy, and disease volume were not. For baseline CAFs, higher levels of lumican, osteopontin, tenascin C, DKK1, TGFβ2, IL6, CXCL5, CD25, CD30, CCL24, IL27, CXCL10, MMP-1, and CD117 were significantly associated with shorter mPFS.

Table 5 presents results for the multivariate Cox model. Although BAP levels were no longer significant, high baseline levels of Lumican (HR, 2.50; 95% CI, 1.32–4.75, $P = 0.005$), CXCL5 (HR, 4.54; 95% CI, 2.09–9.87, $P < 0.001$), CD25 (HR, 2.61; 95% CI, 1.29–5.28, $P = 0.007$), and CD30 (HR, 1.93; 95% CI, 1.03–3.60, $P = 0.039$) remained independently associated with shorter mPFS. A prognostic risk score (0–4) was calculated using the coefficients from the reduced multivariate model. The score was based on the following formula: risk factor score (RFs) $= 0.66 \times$ (CD30 $\geq$ 797) $+ 0.96 \times$ (IL2R $\geq$ 2012) $+ 0.92 \times$ (Lumican $\geq$ 878.91) $+ 1.51 \times$ (ENA78 (CXCL5) $\geq$338).

Figure 1 shows the Kaplan–Meier plot for the score. Changes in CAF concentrations at 6 weeks in response to cabozantinib were not associated with clinical outcome (data not shown).

Discussion

Our results suggest that cabozantinib with plus ADT is an effective combination in patients with HNMPCa. Prior data from our institution showed that the median time to castrate-resistant progression in patients with high-volume disease treated with ADT alone was 11.2 months (11). Thus, the mPFS of 16.1 months we observed in high-volume patients in our study suggests promising anti-disease activity. It is possible that the improved mPFS we observed in the high-volume group with cabozantinib plus ADT relative to the high-volume group treated with ADT alone in our previously published study is due to differences in other relevant prognostic baseline characteristics between the two populations. However, it is worth noting that in the current study, relatively fewer patients had prior definitive local therapy to the prostate (26% vs. 40%) and more patients had baseline PSAs > 20 (74% vs. 56%), two other covariates associated with shorter time to castrate resistance in the earlier study. Based on this, it seems

Table 3. Univariate analysis of baseline markers in tumor tissue.

Molecular marker expression	N (%)	Events	mPFS (months)	HR (95% CI) for HR	P
AR-N presence					
No	2 (11)	2	12.3		
Yes	16 (89)	16	14.8	1.08 (0.24–4.84)	0.919
AR-N, >75%, high intensity					
No	7 (39)	7	12.3		
Yes	11 (61)	11	14.6	0.98 (0.37–2.59)	0.961
NKX3.1 presence					
Yes	20 (100)	18	14.87	1.00 (1.00–1.00)	
CYP17, >25%					
No	12 (60)	10	14.6		
Yes	8 (40)	8	14.9	1.03 (0.39–2.72)	0.953
ARV7 presence					
No	19 (90)	17	15.0		
Yes	2 (10)	2	9.5	2.78 (0.59–13.16)	0.199
GR, >25%					
No	13 (62)	11	16.6		
Yes	8 (38)	8	11.9	1.56 (0.60–4.08)	0.366
Phospho-MET, >75%					
No	15 (75)	13	17.3		
Yes	5 (25)	5	12.3	3.40 (1.07–10.83)	0.039
CD31, >25%					
No	10 (48)	8	17.3		
Yes	11 (52)	11	12.1	3.39 (1.21–9.47)	0.020
Phospho-FGFR1, >25%					
No	13 (65)	11	21.5		
Yes	7 (35)	7	14.5	5.10 (1.45–17.92)	0.011
Ki67, >3%					
No	15 (75)	13	17.3		
Yes	5 (25)	5	9.5	7.23 (1.88–27.85)	0.004

unlikely that differences in baseline characteristics alone could fully account for our positive results.

This clinical efficacy signal supports the hypothesis that therapeutic strategies that target the tumor stroma may improve patient outcomes (19). Our data further suggest that applying stromal targeting therapies earlier in the disease course may potentially enhance efficacy beyond what has been observed in heavily pretreated patients with castrate-resistant disease, the patient group most commonly studied in clinical trials with these agents. Because acquired resistance to androgen deprivation coincides with progression in bone, the predominant site of lethal disease, targeting specific bone stromal–epithelial interactions is of particular interest and impact (20).

Our biomarker data are also consistent with preclinical and coclinical models demonstrating the importance of bone stromal–epithelial interactions in promoting prostate cancer progression and resistance to cabozantinib. Markers of autocrine-paracrine signaling pathways mediating cross-talk between prostate cancer cells and osteoblasts (pFGFR1, Lumican), endothelial cells (pFGFR1), and immune cells (CXCL5, CD25, and CD30) were the strongest predictors of outcome, whereas markers of AR signaling (AR-N, CYP17) and baseline clinical variables (PSA, ECOG, Gleason score, and LDH) that others have previously associated with time to castrate-resistant in response to ADT alone in HNMPCa were not (21). We are not aware of any studies reporting the effects of ADT monotherapy on CAFs in patients with hormone-naïve metastatic prostate cancer. However, we are aware of one study by Saylor and colleagues that examined the effect of ADT monother-

apy on CAFs in hormone-naïve patients with locally advanced or recurrent prostate cancer without bone metastases (22). CAFs analyzed in both studies were VEGF, FGF-2, IL1β, IL6, IL8, TNFα, SDF-1, and sc-Kit. In the study by Saylor and colleagues, only IL6 levels were statistically significantly changed (decreased) from baseline. In contrast, we observed statistically significant changes in VEGF (increased), IL1β (decreased), IL8 (decreased), and sc-Kit (decreased). These results suggest a contribution of cabozantinib to the CAF modulation observed in our study.

The association between high circulating levels of immunomodulatory cytokines and shorter time to castrate resistance is consistent with their shared ability to recruit MDSCs to the tumor microenvironment. In mouse models of prostate adenocarcinoma driven by dual loss of Pten and Smad4, cancer cells secrete CXCL5 to attract CXCR2-expressing MDSCs that contribute to tumor progression (23). IL23 secreted by MDSCs has been shown to promote castrate-resistant progression by activating the androgen receptor pathway in prostate tumor cells in PTEN$^{PC-/-}$ mice (24). Thus, cabozantinib-mediated suppression of CXCL5, IL23, and other "immune-inhibitory" cytokines we observed would theoretically inhibit cross-talk between MDSCs and prostate cancer cells to inhibit tumor growth. Additional studies directly measuring CAFs, their cellular localization, and immune cell function in the bone tumor microenvironment in response to cabozantinib will be required to formally test these hypotheses.

Our results further suggest that optimizing the therapeutic potential of cabozantinib-mediated c-MET/VEGR2 inhibition in HNMPCa will require combinations with agents beyond conventional ADT.

Table 4. Analysis of CAFs.

	n	Baseline Median	IQR		6 weeks Median	IQR		Median fold change	P
Angiogenesis									
HGF pg/mL	54	234.6	180.8	318.9	221.7	161.8	305.1	−0.04	0.2704081
sHGFR/c-MET pg/mL	54	46,061.7	37,295.7	53,821.2	46,644.5	38,269.8	57,912.2	0.04	0.03035172
PLGF pg/mL	54	10.4	6.3	15.1	28.6	18.4	47.5	1.95	6.154e−10
VEGF-A pg/mL	54	72.4	39.2	113.3	137.0	76.5	199.1	0.60	3.948e−07
BMP-9 pg/mL	54	59.0	35.8	89.2	28.9	11.8	43.2	−0.49	2.389e−07
Angiopoietin-2 pg/mL	54	1,281.1	946.4	1,814.4	944.8	715.7	1,407.8	−0.23	3.219e−07
Endoglin pg/mL	54	544.7	368.7	773.3	441.1	301.6	591.2	−0.20	1.727e−06
Bone stromal									
IGF-2 pg/mL	54	179,177.6	95,523.8	303,896.5	348,761.5	228,987.7	493,252.2	0.85	7.389e−08
Galectin-3 ng/mL	54	3.6	2.7	4.5	4.3	3.5	5.6	0.32	1.334e−06
Tenascin C pg/mL	54	12,535.2	9,931.5	14,330.1	14,955.8	10,387.0	18,873.0	0.20	0.00015421
Periostin ng/mL	54	105.9	92.7	158.9	79.5	59.7	95.3	−0.37	2.407e−10
Osteonectin (SPARC) pg/mL	54	203.4	186.2	277.2	173.0	144.4	220.5	−0.16	2.130e−07
OPN (SPP1) pg/mL	54	43,708.2	24,559.6	75,045.0	28,035.2	18,451.9	48,420.5	−0.26	3.525e−07
Lumican ng/mL	54	878.9	716.0	1,034.0	667.6	577.2	821.0	−0.22	1.518e−06
MCP-2/CCL8 pg/mL	54	15.2	8.5	31.3	13.3	6.9	18.4	−0.13	0.0157261
Vitronectin ng/mL	54	42,413.9	37,916.0	46,798.0	43,154.0	39,120.6	49,817.2	0.04	0.15168607
TGFß1 pg/mL	54	7,786.8	5,309.6	12,758.7	5,869.0	4,135.9	12,176.8	−0.09	0.21343461
IGFBP-2 pg/mL	54	6.2	2.6	11.8	2.0	0.9	5.0	−0.58	1.120e−08
DKK1 pg/mL	54	445.5	328.4	696.4	446.8	329.7	720.6	0.01	0.85989371
FGF-1 pg/mL	54	20.8	15.2	28.6	22.2	16.1	29.4	−0.01	0.41091777
FGF-2 pg/mL	54	112.7	87.7	141.3	120.3	104.6	142.4	0.02	0.46162296
IL6 pg/mL	54	299.3	82.9	538.3	193.7	59.6	414.9	0.00	0.12211327
sIL6Ra pg/mL	54	30,511.7	25,336.2	35,046.2	27,300.5	22,674.1	31,909.5	−0.09	6.325e−07
sgp 130 pg/mL	54	80,909.9	66,511.6	91,959.3	78,403.2	63,294.1	88,730.7	−0.04	0.04171858
MMP-9 ng/mL	54	22.7	12.6	38.4	15.3	10.2	29.8	−0.29	0.00874638
Tweak pg/mL	54	4,937.4	2,805.7	8,681.1	3,918.7	2,431.1	6,038.7	−0.04	0.01298983
Immune-inhibitory									
sAXL pg/mL	54	1,828.2	1,241.7	2,307.2	2,300.8	1,634.1	3,239.7	1.35	7.217e−08
MCP-1 (CCL2) pg/mL	54	77.7	56.0	139.0	94.8	67.2	174.1	0.28	0.00366142
sc-Kit/SCFR (CD117) pg/mL	54	27,212.7	23,140.9	3,3803.8	18,769.7	13,857.6	23,571.4	−0.34	5.718e−09
CD30 pg/mL	54	646.2	371.0	952.5	423.1	296.1	618.9	−0.25	2.428e−06
MDC/CCL22 pg/mL	54	148.0	94.8	247.4	99.7	51.8	165.6	−0.24	0.00001875
IL2R (CD25) pg/mL	54	1,377.9	874.7	2,022.9	1,157.1	507.6	1,660.3	−0.22	0.00011664
IL1 alpha pg/mL	54	12.9	6.9	20.8	9.5	4.7	17.1	−0.18	0.01108405
IL1 beta pg/mL	54	20.9	8.2	49.5	16.1	4.7	29.6	−0.20	0.04669541
IL8 (CXCL8)pg/mL	54	40.8	20.2	76.5	23.7	15.2	54.4	−0.22	0.00276356
IL9 pg/mL	54	34.9	15.3	68.3	21.7	12.7	54.8	−0.09	0.03303796
IL10 pg/mL	54	29.2	17.4	61.0	17.6	15.0	52.0	−0.15	0.03555636
IL13 pg/mL	54	63.2	31.1	82.5	47.4	27.6	68.8	−0.09	0.03919372
IL18 pg/mL	54	236.7	119.1	323.3	149.8	101.7	274.1	−0.06	0.03380259
IL21 pg/mL	54	104.1	33.4	162.8	64.8	32.5	139.4	−0.16	0.02690257
IL22 pg/mL	54	225.2	94.5	383.9	161.2	65.5	294.0	−0.11	0.02199674
IL23 pg/mL	54	279.5	177.8	417.7	219.1	162.3	354.3	−0.17	0.00659715
TNF-RII pg/mL	54	31.2	20.9	44.2	24.8	16.9	32.5	−0.16	0.00020294
APRIL pg/mL	54	1,324.5	777.3	2,147.9	1,062.0	451.0	1,768.1	−0.16	0.00032468
BAFF pg/mL	54	21.4	6.0	44.7	10.8	5.5	35.3	−0.07	0.02250035
M-CSF pg/mL	54	45.0	13.7	113.2	23.2	8.3	68.1	−0.21	0.00101901
GRO-alpha (CXCL1) pg/mL	54	27.3	13.6	46.6	19.7	11.1	33.4	−0.03	0.03919372
ENA78 (CXCL5) pg/mL	54	247.2	152.7	323.9	190.8	138.7	244.6	−0.08	0.01610374
I-TAC (CXCL11) pg/mL	54	163.7	97.5	317.9	106.0	36.9	201.0	−0.19	0.0035576
TIMP-1 pg/mL	54	39.4	35.2	46.1	35.8	30.2	45.7	−0.06	0.00800232
Immune-stimulatory									
Eotaxin-1 (CCL11) pg/mL	54	28.8	20.9	38.6	34.2	22.4	45.1	0.20	0.00520579
IL2 pg/mL	54	9.8	6.1	17.0	9.6	5.9	14.7	0.07	0.49636927
TNF-alpha pg/mL	54	35.6	18.4	60.7	32.4	15.5	48.8	0.02	0.85313516
IFN-gamma pg/mL	54	71.8	34.5	129.1	51.2	25.3	103.6	−0.11	0.03679983
IL15 pg/mL	54	35.7	8.3	55.9	25.1	13.2	46.1	−0.12	0.01265394
TRAIL pg/mL	54	41.4	21.1	71.9	30.9	16.6	54.8	−0.06	0.03679983
IL27 pg/mL	54	149.1	72.5	300.3	120.4	61.2	185.9	−0.19	0.04043759
IL12p70 pg/mL	54	5.9	2.3	11.3	4.1	2.5	8.5	−0.12	0.04576123

Table 5. Multivariate analysis for PFS.

Cytokine and angiogenic factor	N	Events	mPFS (months)	HR (95% CI) for HR	P
[a]Lumican ng/mL					
<878.91	30	19	20.2		
≥878.91	30	29	14.3	2.50 (1.32–4.75)	0.005
[a]ENA78 (CXCL5) pg/mL					
<338	47	35	20.2		
≥338	13	13	9.9	4.54 (2.09–9.87)	<0.001
[b]IL2R (CD25) pg/mL					
<2012	43	32	21.4		
≥2012	17	16	11.1	2.61 (1.29–5.28)	0.007
[b]CD30 pg/mL					
<797	38	28	21.4		
≥797	22	20	9.9	1.93 (1.03–3.60)	0.039

[a]Cutoff was median.
[b]Cutoff was CART.

Candidate pathways for cotargeting with c-MET/VEGR2 blockade include inhibitors of CYP17-mediated androgen biosynthesis, FGF/FGFR signaling, integrin signaling, and immune checkpoints. While our study was being conducted, three phase III clinical trials (CHAARTED, LATITUDE, and STAMPEDE) demonstrated that the efficacy (PFS and OS) of docetaxel and abiraterone acetate in mCRPC was enhanced when given in HNMPCa (25–28). Though comparisons across studies can be challenging for a variety of reasons (e.g., differences in patient populations, definitions of disease volume, and study design), we would predict that docetaxel and abiraterone are superior to cabozantinib in benefiting patients with hormone-naïve disease. For example, the median radiographic PFS was observed in our study was greater than the control (ADT alone) arm of LATITUDE but less than the abiraterone arm (compare 17.7 vs. 14.8 vs. 33.0 months). However, the efficacy signal we sought to explore as a primary objective in our study (designed prior to CHAARTED, LATTITUDE, and STAMPEDE) was based on the hypothesis that inhibiting stromal pathways in bone would enhance the efficacy of

conventional androgen ablation. Based on historical data from our group looking at patients treated with ADT alone, we conclude our data support this hypothesis. Moving forward, therefore, we postulate that "stromal-targeting" agents that inhibit c-MET/VEGFR2 signaling could enhance the efficacy of more potential "epithelial-targeting" agents including docetaxel and abiraterone. Cotargeting the stromal and epithelial compartments provides a conceptual framework for possibly enhancing the current epithelial-targeting paradigm with the expectation of proportionally greater benefit in the hormone-naïve versus castration-resistant disease state.

The benefits of using cabozantinib in HNMPCa need to be considered with the potential for increased toxicity. In a prior study of cabozantinib in mCRPC using a starting dose of 100 mg daily, 84% of patients required a dose reduction and 25% discontinued treatment secondary to an adverse event (1). At a starting dose of 60 mg daily in our study, the incidence of treatment discontinuation was slightly less at 16%, but dose reductions still occurred in 85% of patients. One possible reason for this is the greater duration of time patients in our

Figure 1.
PFS according to 4 baseline risk factors (RF): high Lumican (above the median), high CXCL5 (above CART cutoff), high CD25 (above CART cutoff), and high CD30 (above CART cutoff). PFS curves were generated for patients falling into 5 separate risk groups: 0, 1, 2, 3, and 4 RFs. Only 1 patient had all 4 RFs.
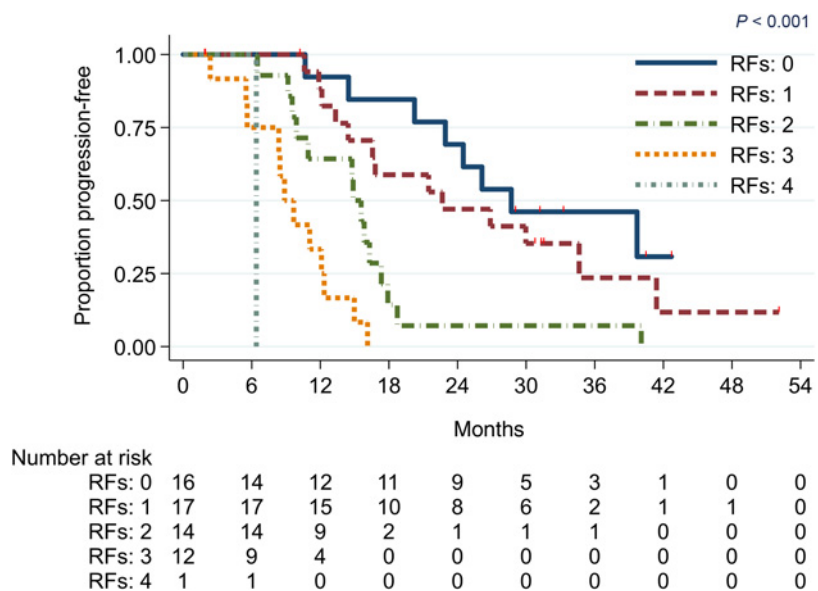
study received cabozantinib. The median duration of cabozantinib treatment was 13.8 months, the longest in the published literature compared with clinical trials in mCRPC (median 5.0 months in COMET-1), medullary thyroid cancer (6.8 months), and kidney cancer (median 8.3 months; refs. 2, 29, 30). Thus, although there were no unexpected safety concerns, the fact that HNMPCa patients may benefit longer from cabozantinib needs to be anticipated in the design of future trials. One strategy to address this is to move toward dose individualization of tyrosine kinase inhibitors (TKI; ref. 31). As there are no TKIs approved for prostate cancer, the experience with modifications in dose and schedule comes principally from other tumor types including chronic myelogenous leukemia (dasatinib or nilotinib) and metastatic kidney cancer (sunitinib). Retrospective studies from our institution suggest that dose modifications and alterations in schedule do not compromise efficacy and enhance patient safety, quality of life, and dose intensity (by virtue of continuing treatment for longer periods of time with adequate drug exposure; refs.13–15). We explored dose individualization in the current study and achieved a median percentage dose density comparable to COMET-1 (compare 69% vs. 75%), even though patients in our study were on cabozantinib considerably longer when prohibitive cumulative toxicities from TKIs are expected to occur. Given the relatively long half-life of cabozantinib (55 hours), dose individualization may be particularly applicable. Prospective studies will be needed to further test and validate this strategy.

A limitation of our study is the single-arm design. A single-arm study confounds the ability to distinguish whether baseline clinical features or potential biomarkers are predictive, prognostic, or both. Molecular-pathologic characterization of prostate cancer as a platform to identify predictive markers is further challenged by the relatively low yield of trans-iliac biopsies for informative tumor material (∼30% in our study), an effort that can be enhanced with image-guided techniques producing higher yields (60%–70%). Thus, our biomarker results are exploratory and moving forward, randomized trials with image-guided and "liquid" biopsies should prove most useful in exploring the potential of therapeutic strategies that inhibit c-MET/VEGF2 signaling in HNMPCa.

In summary, cabozantinib combined with ADT is potently active in HNMPCa. Importantly, our study is the first to report tissue and blood biomarkers that correlate with benefit. Although we and others have previously studied molecular markers and CAFs in clinical trials of cabozantinib in mCRPC, no associations of these markers with clinical benefit were observed (4, 32). This is likely due to the fact that we included novel candidate stromal cell markers in the current study that were informed by prior preclinical and coclinical studies in our group elucidating cabozantinib mechanism of action. Our clinical results and tissue and blood-based research approach to identify predictors of outcome suggest a path forward to develop cabozantinib-based therapeutic strategies that cotarget bone stroma and prostate cancer epithelial cells in a manner that may overcome limitations of the negative phase III study.

Disclosure of Potential Conflicts of Interest

Authors' Contributions

Conception and design: P.G. Corn, C. Logothetis, G. Gallick
Development of methodology: P.G. Corn, L. Xiao, A.J. Zurita, S.-M. Tu, S. Huang, C. Logothetis, G. Gallick
Acquisition of data (provided animals, acquired and managed patients, provided facilities, etc.): P.G. Corn, M. Zhang, A.J. Zurita, S.K. Subudhi, S.-M. Tu, A.M. Aparicio, S. Huang, N.M. Navone, S. Ramachandran, M.A. Titus, E. Efstathiou, P. Troncoso
Analysis and interpretation of data (e.g., statistical analysis, biostatistics, computational analysis): P.G. Corn, M. Zhang, G.M. Nogueras-Gonzalez, L. Xiao, C. Coarfa, K. Rajapakshe, S. Ramachandran, M.A. Titus, E. Efstathiou, P. Troncoso, C. Logothetis, G. Gallick
Writing, review, and/or revision of the manuscript: P.G. Corn, M. Zhang, G.M. Nogueras-Gonzalez, L. Xiao, A.J. Zurita, S.K. Subudhi, S.-M. Tu, A.M. Aparicio, S. Huang, N.M. Navone, S.-H. Lin, G. Wang, T. Panaretakis, E. Efstathiou, P. Troncoso, C. Logothetis, G. Gallick
Administrative, technical, or material support (i.e., reporting or organizing data, constructing databases): P.G. Corn
Study supervision: P.G. Corn
Other (e.g., expert testimony): S.-M. Tu

Acknowledgments

References

1. Smith MR, Sweeney CJ, Corn PG, Rathkopf DE, Smith DC, Hussain M, et al. Cabozantinib in chemotherapy-pretreated metastatic castration-resistant prostate cancer: results of a phase II nonrandomized expansion study. J Clin Oncol 2014;32:3391–9.
2. Smith M, De Bono J, Sternberg C, Le Moulec S, Oudard S, De Giorgi U, et al. Phase III study of cabozantinib in previously treated metastatic castration-resistant prostate cancer: COMET-1. J Clin Oncol 2016;34:3005–13.
3. Lee YC, Lin SC, Yu G, Cheng CJ, Bin Liu B, Liu HC, et al. Identification of bone-derived factors conferring de novo therapeutic resistance in metastatic prostate cancer. Cancer Res 2015;75:4949–59.
4. Varkaris A, Corn PG, Parikh NU, Efstathiou E, Song JH, Lee YC, et al. Integrating murine and clinical trials with cabozantinib to understand roles of MET and VEGFR2 as targets for growth inhibition of prostate cancer. Clin Cancer Res 2016;22:107–21.
5. Yu KJ, Li JK, Lee YC, Yu G, Lin SC, Pan T, et al. Cabozantinib-induced osteoblast secretome promotes survival and migration of metastatic prostate cancer cells in bone. Oncotarget 2017;8:74987–5006.
6. Verras M, Lee J, Xue H, Li TH, Wang Y, Sun Z. The androgen receptor negatively regulates the expression of c-Met: implications for a novel mechanism of prostate cancer progression. Cancer Res 2007; 67:967–75.
7. Maeda A, Nakashiro K, Hara S, Sasaki T, Miwa Y, Tanji N, et al. Inactivation of AR activates HGF/c-Met system in human prostatic carcinoma cells. Biochem Biophys Res Commun 2006;347:1158–65.

8. Knudsen BS, Gmyrek GA, Inra J, Scherr DS, Vaughn ED, Nanus DM, et al. High expression of the Met receptor in prostate cancer metastasis to bone. Urology 2002;60:1113–7.

9. Verhoef EI, Kolijn K, De Herdt MJ, van der Steen B, Hoogland AM, Sleddens HF, et al. MET expression during prostate cancer progression. Oncotarget 2016;7: 31029–36.

10. Qiao Y, Feng FY, Wang Y, Cao X, Han S, Wilder-Romans K, et al. Mechanistic support for combined MET and AR blockade in castration-resistant prostate cancer. Neoplasia 2016;18:1–9.

11. Millikan RE, Wen S, Pagliaro LC, Brown MA, Moomey B, Do KA, et al. Phase III trial of androgen ablation with or without three cycles of systemic chemotherapy for advanced prostate cancer. J Clin Oncol 2008;26:5936–42.

12. Kyriakopoulos CE, Chen YH, Carducci MA, Liu G, Jarrard DF, Hahn NH, et al. Chemohormonal therapy in metastatic hormone-sensitive prostate cancer: long-term survival analysis of the randomized phase III E3805 CHAARTED Trial. J Clin Oncol 2018;36:1080–7.

13. Atkinson BJ, Kalra S, Wang X, Bathala T, Corn P, Tannir NM, et al. Clinical outcomes in metastatic renal cell carcinoma patients treated with alternative sunitinib schedules. J Urol 2014;191:611–8.

14. Jonasch E, Slack RS, Geynisman DM, Hasanov E, Milowsky MI, Rathmell WK, et al. Phase II study of two weeks on, one week off sunitinib scheduling in patients with metastatic renal cell carcinoma. J Clin Oncol 2018;36: 1588–93.

15. Santos FPS, Kantarjian H, Fava C, O'Brien S, Garcia-Manero G, Ravandi F, et al. Clinical impact of dose reductions and interruptions of second-generation tyrosine kinase inhibitors in patients with chronic myeloid leukaemia. Br J Haematol 2010;150:303–12.

16. Titus MA, Schell MJ, Lih FB, Tomer KB, Mohler JL. Testosterone and dihydrotestosterone tissue levels in recurrent prostate cancer. Clin Cancer Res 2005; 11:4653–7.

17. Msaouel P, Zurita AJ, Huang S, Jonasch E, Tannir NM. Plasma cytokine and angiogenic factors associated with prognosis and therapeutic response to sunitinib vs. everolimus in advanced non-clear cell renal cell carcinoma. Oncotarget 2017;8:42149–58.

18. Dayyani F, Zurita AJ, Nogueras-González GM, Slack R, Millikan RE, Araujo JC, et al. The combination of serum insulin, osteopontin, and hepatocyte growth factor predicts time to castration-resistant progression in androgen dependent metastatic prostate cancer- an exploratory study. BMC Cancer 2016;16:721.

19. Valkenburg KC, de Groot AE, Pienta KC. Targeting the tumour stroma to improve cancer therapy. Nat Rev Clin Oncol 2018;15:366–81.

20. Logothetis CJ, Gallick GE, Maity SN, Kim J, Aparicio A, Efstathiou E, et al. Molecular classification of prostate cancer progression: foundation for marker-driven treatment of prostate cancer. Cancer Discov 2013;3: 849–61.

21. Grivas PD, Robins DM, Hussain M. Predicting response to hormonal therapy and survival in men with hormone sensitive metastatic prostate cancer. Crit Rev Oncol Hematol 2013;85:82–93.

22. Saylor P, Kozak KR, Smith MR, Ancukiewicz MA, Efstathiou JA, et al. Changes in biomarkers of inflammation and angiogenesis during androgen deprivation therapy for prostate cancer. Oncologist 2012;17:212–9.

23. Wang G, Lu X, Dey P, Deng P, Wu CC, Jiang S, et al. Targeting YAP-dependent MDSC infiltration impairs tumor progression. Cancer Discov 2016;6:80–95.

24. Calcinotto A, Spataro C, Zagato E, Di Mitri D, Gil V, Crespo M, et al. IL-23 secreted by myeloid cells drives castration-resistant prostate cancer. Nature 2018;559:363–9.

25. Sweeney CJ, Chen YH, Carducci M, Liu G, Jarrard DF, Eisenberger M, et al. Chemohormonal therapy in metastatic hormone-sensitive prostate cancer. N Engl J Med 2015;373:737–46.

26. James ND, Sydes MR, Clarke NW, Mason MD, Dearnaley DP, Spears MR, et al. Addition of docetaxel, zoledronic acid, or both to first-line long-term hormone therapy in prostate cancer (STAMPEDE): survival results from an adaptive, multi-arm, multistage, platform randomised controlled trial. Lancet 2016;387:1163–77.

27. Fizazi K, Tran N, Fein L, Matsubara N, Rodriguez-Antolin A, Alekseev BY, et al. Abiraterone plus prednisone in metastatic, castration-sensitive prostate cancer. N Engl J Med 2017;377:352–60.

28. James ND, de Bono JS, Spears MR, Clarke NW, Mason MD, Dearnaley DP, et al. Abiraterone for prostate cancer not previously treated with hormone therapy. N Engl J Med 2017;377:338–51.

29. Elisei R, Schlumberger MJ, Muller SP, Schoffski P, Brose MS, Shah MH, et al. Cabozantinib in progressive medullary thyroid cancer. J Clin Oncol 2013;31:3639–46.

30. Choueiri TK, Escudier B, Powles T, Tannir NM, Mainwaring PN, Rini BI, et al. Cabozantinib versus everolimus in advanced renal cell carcinoma (METEOR): final results from a randomised, open-label, phase 3 trial. Lancet Oncol 2016;17: 917–27.

31. Klümpen HJ, Samer CF, Mathijssen RHJ, Schellens JHM, Gurney H. Moving towards dose individualization of tyrosine kinase inhibitors. Cancer Treat Rev 2011;37:251–60.

32. Leibowitz-Amit R, Pintilie M, Khoja L, Azad AA, Berger R, Laird AD, et al. Changes in plasma biomarkers following treatment with cabozantinib in metastatic castration-resistant prostate cancer: a post hoc analysis of an extension cohort of a phase II trial. J Transl Med 2016;14:12.